

# Liver X Receptor Is a Therapeutic Target for Photoaging and Chronological Skin Aging

Ken C. N. Chang, Qi Shen, Inn Gyung Oh, Scott A. Jelinsky, Susan F. Jenkins, Wei Wang, Yihe Wang, Margaret LaCava, Matthew R. Yudt, Catherine C. Thompson, Leonard P. Freedman, Jin Ho Chung, and Sunil Nagpal

*Nuclear Receptors and Dermatology (K.C.N.C., Q.S., S.A.J., S.F.J., W.W., Y.W., M.L., M.R.Y., C.C.T., L.P.F., S.N.), Women's Health and Musculoskeletal Biology, Wyeth Research, Collegeville, Pennsylvania 19426; and Laboratory of Cutaneous Aging Research (I.G.O., J.H.C.), Department of Dermatology, Seoul National University College of Medicine, Seoul National University, Seoul 110-744, Republic of Korea.*

Liver X receptors (LXR $\alpha$  and  $\beta$ ) are liposensors that exert their metabolic effects by orchestrating the expression of macrophage genes involved in lipid metabolism and inflammation. LXRs are also expressed in other tissues, including skin, where their natural oxysterol ligands induce keratinocyte differentiation and improve epidermal barrier function. To extend the potential use of LXR ligands to dermatological indications, we explored the possibility of using LXR as a target for skin aging. We demonstrate that LXR signaling is down-regulated in cell-based models of photoaging, *i.e.* UV-activated keratinocytes and TNF $\alpha$ -activated dermal fibroblasts. We show that a synthetic LXR ligand inhibits the expression of cytokines and metalloproteinases in these *in vitro* models, thus indicating its potential in decreasing cutaneous inflam-

mation associated with the etiology of photoaging. Furthermore, a synthetic LXR ligand induces the expression of differentiation markers, ceramide biosynthesis enzymes, and lipid synthesis and transport genes in keratinocytes. Remarkably, LXR $\beta$ -null mouse skin showed some of the molecular defects that are observed in chronologically aged human skin. Finally, we demonstrate that a synthetic LXR agonist inhibits UV-induced photo-damage and skin wrinkle formation in a murine model of photoaging. Therefore, the ability of an LXR ligand to modulate multiple pathways underlying the etiology of skin aging suggests that LXR is a novel target for developing potential therapeutics for photoaging and chronological skin aging indications. (*Molecular Endocrinology* 22: 2407–2419, 2008)

SKIN AGING IS a result of the combination of two biological processes, chronological aging and photoaging. Chronological aging represents the physiological changes in skin that occur over time, resulting in a dry, thin skin that has fine wrinkles and is easily injured. Photoaging results from the damaging effects of solar UV radiation, causing the skin to age prematurely, and is characterized by wrinkles, laxity, and dryness (1–3). Some of the molecular mechanisms underlying skin aging have been uncovered. The pro-

cess of photoaging involves epidermal keratinocytes, dermal fibroblasts, and infiltrating neutrophils. UV exposure induces activator protein 1 (AP-1) and nuclear factor- $\kappa$ B (NF- $\kappa$ B) activation in the skin, leading to the expression of matrix metalloproteinases (MMPs) and cytokines in keratinocytes (4). Cytokines in turn activate dermal fibroblasts to secrete MMPs, which damage the extracellular matrix (5). Cytokines and other chemotactic factors also recruit neutrophilic granulocytes to the dermis, which secrete elastase and MMPs, thus contributing to UV-mediated dermal extracellular matrix degradation (3). Repeated exposure to UV radiation results in the accumulation of incompletely degraded collagen in the dermis, leading to wrinkle formation. Chronological aging is characterized by cellular senescence, leading to decreased keratinocyte proliferation, improper terminal differentiation, reduced neutral lipid synthesis, and reduced collagen synthesis (6–11). Prostaglandin E2 (PGE2), MMP production, and oxidative damage are also increased (10, 12–14). Agents that inhibit one or more of these processes are candidates for a therapeutic target for skin aging.

Liver X receptors (LXR $\alpha$ /NR1H3 and LXR $\beta$ /NR1H2) are ligand-dependent transcription factors whose

## First Published Online September 11, 2008

Abbreviations: AP-1, Activator protein 1; COX-2, cyclooxygenase-2; ER, estrogen receptor; FLG, filaggrin; IVL, involucrin; KO, knockout; LASS, ceramide synthase; LBD, ligand binding domain; LOR, loricrin; LXR, liver X receptor; MED, minimum erythema dose; MMP, matrix metalloproteinase; NF- $\kappa$ B, nuclear factor- $\kappa$ B; NHDF, normal human dermal fibroblast; NHEK, normal human epidermal keratinocyte; NR, nuclear receptor; PGE2, prostaglandin E2; PPAR, peroxisome proliferator-activated receptor; PTGES, prostaglandin E synthase; RAR, retinoic acid receptor; SMPD, sphingomyelin phosphodiesterase; TGM, transglutaminase; TIMP, tissue inhibitor of metalloproteinases; TLDA, TaqMan low-density array; VDR, vitamin D receptor; WT, wild type.

**Molecular Endocrinology** is published monthly by The Endocrine Society (<http://www.endo-society.org>), the foremost professional society serving the endocrine community.

agonists induce the expression of genes involved in cholesterol efflux and transport and decrease the expression of inflammatory mediators in macrophages and microglia (15–17). These activities underlie the atheroprotective and anti-Alzheimer's potential of LXR ligands (17–19). In addition, LXR agonists display potent antiinflammatory activities and have shown therapeutic efficacy in murine models of dermatitis and rheumatoid arthritis (20, 21). In the skin, LXRs are expressed in keratinocytes (LXR $\alpha$  and  $\beta$  in human and LXR $\beta$  in murine keratinocytes), and their natural ligands have been shown to induce keratinocyte differentiation (21, 22) and improve epidermal barrier function (23). The synthetic ligand (T1317) used in this study (24) has been shown to induce ABCA1 expression in human keratinocytes and murine skin (25). It also induced the expression of AP1 protein, Fra-1, in keratinocytes (26) and stimulated epidermal lipid synthesis in murine skin (23). Based on these properties, we hypothesized that an LXR ligand could interfere with various steps involved in the etiology of both photoaging and chronological skin aging. Therefore, we examined the effects of a synthetic LXR ligand in models of skin aging using keratinocytes and fibroblasts as well as in a murine model of photoaging. Our observations indicate that LXR ligands could provide a new category of therapeutic agents for both photoaging and chronological skin aging.

## RESULTS

### LXR Signaling in Cell-Based Systems of Photoaging

LXR $\beta$  was the predominant isoform in normal human epidermal keratinocytes (NHEKs), whereas both LXR $\alpha$  and  $\beta$  were equally expressed in dermal HFF fibroblasts (Fig. 1A). For comparison purposes, the expression of vitamin D receptor (VDR) in both NHEKs and dermal fibroblasts is also shown (Fig. 1A). We next examined the expression of LXR $\alpha$  and  $\beta$  in various human tissues by *in silico* data mining of an internally derived database of Affymetrix Human Genome U133 Plus 2.0 microarray data. The collection consisted of approximately 8000 individual samples representing 33 distinct tissues. As shown in Fig. 1, B and C, both LXR $\alpha$  and  $\beta$  were expressed in human skin (*black bars*) and a number of other tissues. Notably, LXR $\beta$  was the predominant isotype expressed in human white blood cells and neutrophils (Fig. 1C; *gray bars*), a cell type that is implicated in photoaging (3). Because UV exposure of epidermal keratinocytes and cytokine activation of dermal fibroblasts are postulated to be the initial triggering events in photoaging (5), status of the LXR signaling pathway was studied after these treatments. In NHEKs, UV radiation inhibited the expression of known LXR-responsive genes while at the same time induced the expression of

MMP1 (Fig. 1D). Similarly, TNF $\alpha$  treatment of normal human dermal fibroblasts (NHDFs) and a dermal fibroblast cell line (BJ) also decreased the expression of the known LXR-responsive genes (Fig. 1, E and F). In addition, TNF $\alpha$  treatment induced the expression of MMP1, ADAMTS4, and prostaglandin E synthase (PTGES) in fibroblasts (Fig. 1, E and F). These results indicate that the UV and cytokine activation of skin cells not only induces the expression of inflammation-related MMP1, ADAMTS4, and PTGES genes but also represses the expression of classical LXR-responsive genes.

### Identification of LXR as a Target for Photoaging

To evaluate LXR as a target for photoaging, NHEKs were treated with vehicle or a synthetic LXR ligand (T1317) (24) with or without UV radiation (8 mJ/cm<sup>2</sup>). T1317 was also tested for nuclear receptor (NR) specificity in a biochemical NR-cofactor peptide recruitment assay that provides a readout of the binding of the compound to the NR ligand-binding domain (LBD). In this surrogate ligand binding assay, T1317 recruited cofactor peptides to LXR $\alpha$ , LXR $\beta$ , and pregnane X receptor (PXR) LBD proteins with EC<sub>50</sub> (concentration of the ligand required for 50% increase in NR-cofactor peptide interaction) values of 75, 21, and 7 nM, respectively. T1317 was not active (EC<sub>50</sub> >50  $\mu$ M) in recruiting cofactor peptides to androgen receptor (AR), constitutive androstane receptor (CAR), estrogen receptor- $\alpha$  (ER $\alpha$ ), ER $\beta$ , glucocorticoid receptor, FXR, ER-related receptor- $\alpha$  (ERR- $\alpha$ ), peroxisome proliferator-activated receptor- $\alpha$  (PPAR $\alpha$ ), PPAR $\beta$ , PPAR $\gamma$ , progesterone receptor (PR), retinoic acid receptor- $\alpha$  (RAR $\alpha$ ), RAR $\beta$ , RAR $\gamma$ , retinoid X receptor- $\alpha$  (RXR $\alpha$ ), RXR $\beta$ , thyroid hormone receptor- $\alpha$  (TR $\alpha$ ), TR $\beta$ , and VDR LBD proteins in this ligand-sensing assay. Because pregnane X receptor (PXR) is not expressed in skin, keratinocytes, and dermal fibroblasts (data not shown), T1317 could function only through LXRs in skin systems. UV exposure decreased the expression of LXR $\alpha$  in keratinocytes, which was restored by T1317 treatment (Fig. 2A). In NHEKs, UV-induced expression of TNF $\alpha$ , IL-8, and MMP3 was significantly down-regulated by T1317 (Fig. 2A). Interestingly, significant induction of tissue inhibitor of metalloproteinases (TIMP)-1 expression by the LXR ligand was observed in both mock-exposed and UV-exposed keratinocytes (Fig. 2A). Because UV-exposed keratinocyte cytokines activate dermal fibroblasts by a paracrine pathway in photoaging (5), we next examined the effect of T1317 on cytokine/MMP expression in TNF $\alpha$ -activated fibroblasts. TNF $\alpha$  augmented the expression of MMP1 and MMP3 in BJ fibroblasts, which was significantly inhibited after treatment with the LXR ligand (Fig. 2B). As observed in keratinocytes, fibroblasts also showed the induction of TIMP-1 expression by the LXR ligand in TNF $\alpha$ -treated cells (Fig. 2B). In addition to MMP1 and -3, the LXR ligand also decreased the expression of cyclooxygenase-2 (COX-2)

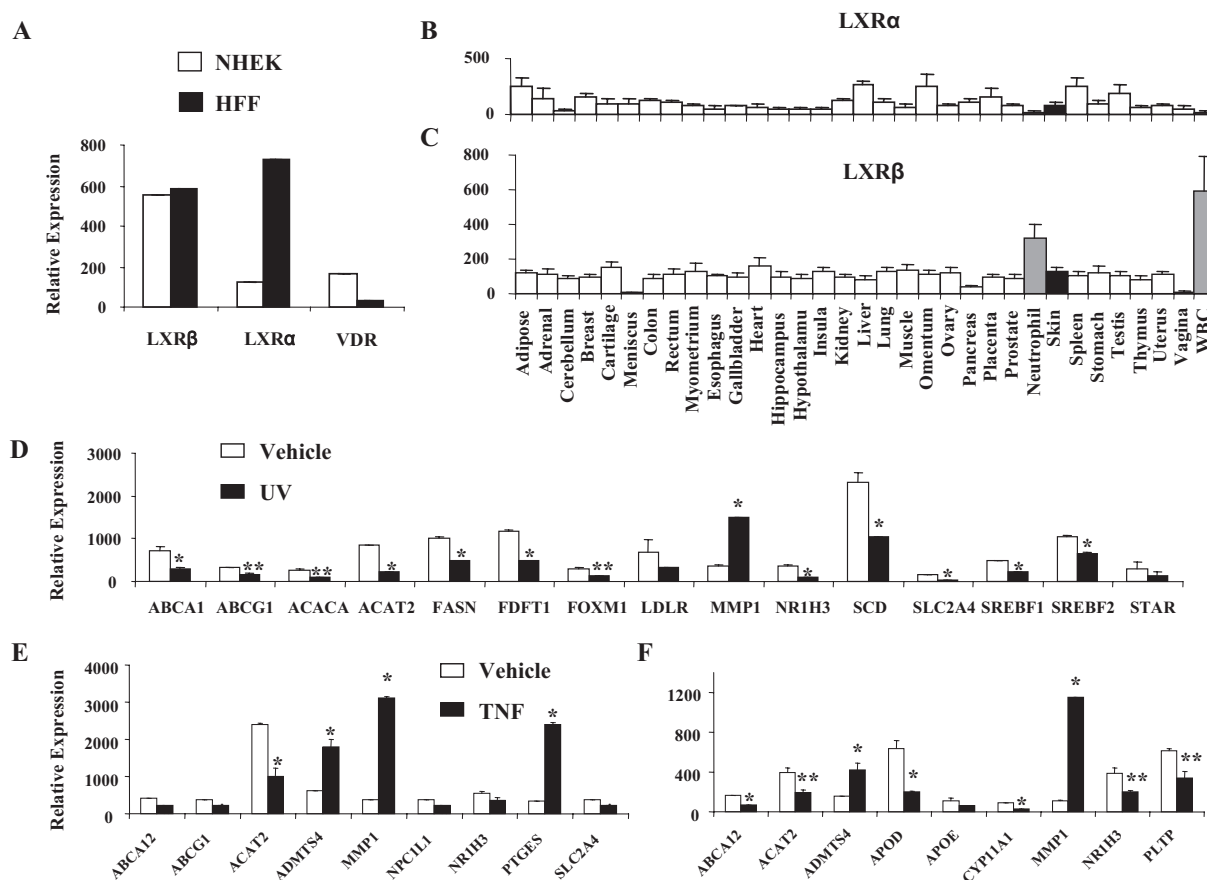


**Fig. 1.** Receptor Expression and the Status of LXR Signaling in Cell-Based Models of Photoaging

A, Relative gene expression levels of LXR $\alpha$ , LXR $\beta$ , and VDR in NHEK (white bars) and HFF (black bars) cells. The expression of these nuclear receptors was measured by real time quantitative PCR; results were normalized to 18S RNA. B and C, Relative expression of LXR $\alpha$  (B) and LXR $\beta$  (C) in various human tissues as analyzed from an internal database derived from Affymetrix Human Genome U133 2.0 Plus data. Black bars represent relative *in silico* expression in skin, and gray bars show the expression of LXR $\beta$  in neutrophils and white blood cells. D, The relative expression level of known LXR-regulated genes and MMP1 was compared in NHEKs with (black bars) or without (white bars) UV exposure (8 mJ/cm<sup>2</sup>) by custom-made TLDA. E, The relative expression of known LXR-regulated genes MMP1, ADAMTS4, and PTGES was compared in NHDFs with (black bars) or without (white bars) TNF $\alpha$  (1 ng/ml) treatment by TLDA used in D. F, The relative expression level of known LXR-regulated genes MMP1, ADAMTS4, and PTGES was compared in BJ fibroblasts with (black bars) or without (white bars) TNF $\alpha$  (1 ng/ml) treatment by TLDA. \*,  $P < 0.01$ ; \*\*,  $P < 0.05$  vs. vehicle control as determined by Student's *t* test.

and cytokines IL-8, IL-6, and IL-1 $\beta$  in TNF $\alpha$ -activated NHDFs (Fig. 2C). Similar results were obtained in TNF $\alpha$ -activated BJ and HFF cells lines (data not shown). To ascertain the receptor specificity of T1317 effects on cytokine/MMP expression, mouse LXR $\beta$  wild-type (WT) or knockout (KO) dermal fibroblasts were used. Cultured LXR $\beta$  WT fibroblasts showed high expression levels of Mmp13 (mouse equivalent of human MMP1), Mmp3, and Il1 $\beta$ . T1317 significantly decreased the expression of these cytokines in WT but not LXR $\beta$  KO fibroblasts, thus indicating that T1317 mediates negative regulation of cytokine/MMP expression through the LXR $\beta$  signaling pathway (Fig. 2D). UV exposure of hairless mice results in epidermal hyperplasia, wrinkle formation, and increased expression of MMP2 and MMP9 (27), and UV also induces these MMPs in human skin (4). Because the expres-

sion of these MMPs was low in cultured human and murine fibroblasts with or without TNF $\alpha$  activation, their expression was analyzed in LXR $\beta$  KO and WT mouse skin. As shown in Fig. 2E, the expression of Mmp2 and Mmp9 was significantly increased in LXR $\beta$  KO mouse skin, thus indicating that the presence of LXR $\beta$  in skin enforces a repression on the expression of these metalloproteinases. These results in UV-exposed keratinocytes, TNF $\alpha$ -activated fibroblasts, and LXR $\beta$  KO fibroblasts and skin samples suggest that LXR is a novel target for photoaging.

#### LXR-Mediated Regulation of Keratinocyte Differentiation Markers

Chronological aging involves defects in keratinocyte terminal differentiation, epidermal barrier repair, and

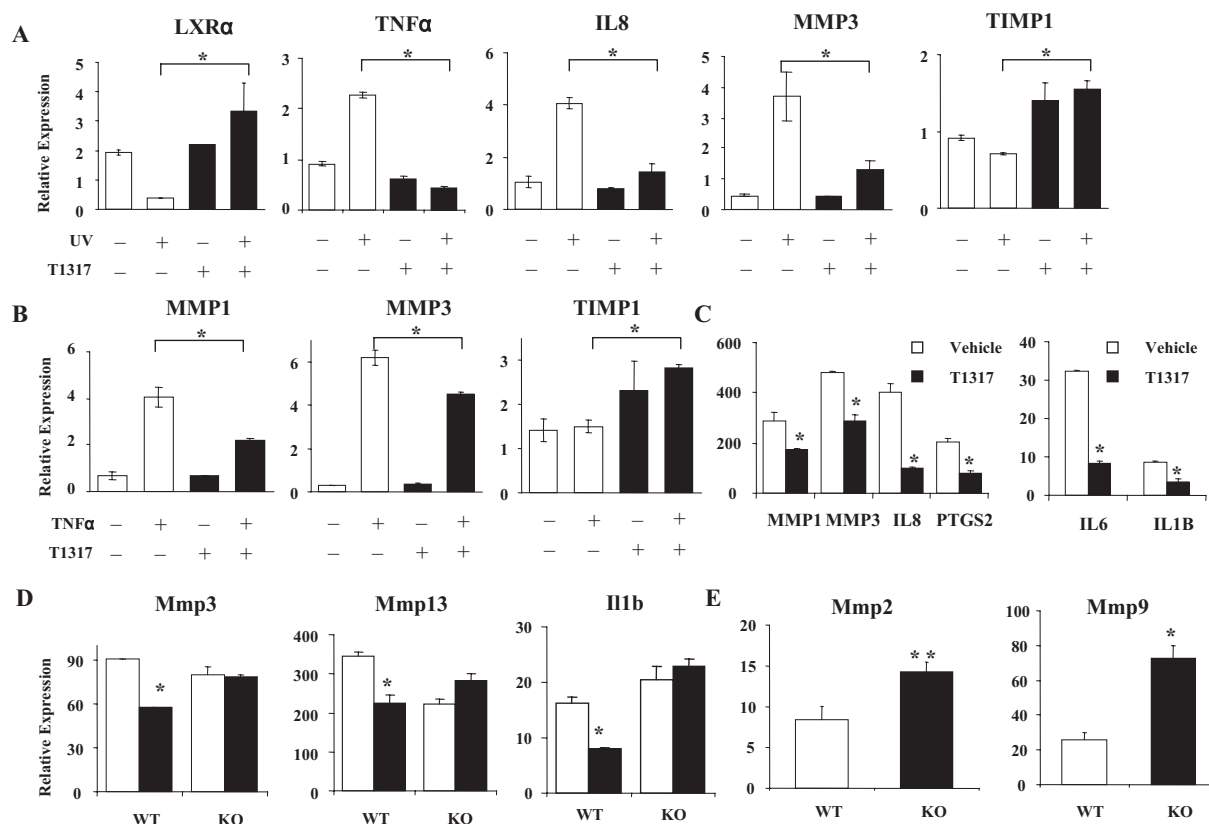


**Fig. 2.** The LXR Ligand Antagonizes UV and Cytokine-Mediated Gene Expression in Skin Cells

A, T1317 inhibits UV activation of keratinocytes. Relative gene expression levels of LXR $\alpha$ , TNF $\alpha$ , IL-8, MMP3, and TIMP1 in NHEKs with and without UV (8 mJ/cm<sup>2</sup>) radiation, in the presence and absence of the synthetic LXR ligand T1317 (1  $\mu$ M). Mean expression of these genes was determined by real-time RT-PCR, and the results were normalized to 18S RNA expression. B, T1317 inhibits cytokine and MMP expression in TNF $\alpha$ -activated dermal fibroblasts. Relative expression levels of MMP1, MMP3, and TIMP1 in BJ fibroblasts with or without TNF $\alpha$  (1 ng/ml) in the presence (black bars) or absence (white bars) of T1317 (1  $\mu$ M) is shown. C, The effect of T1317 on relative gene expression levels of MMP1, MMP3, cytokines (IL-1 $\beta$ , IL-6, and IL-8) and COX-2 in TNF $\alpha$ -treated (1 ng/ml) NHDFs are presented. The relative gene expression levels for these MMP, cytokine, and COX-2 genes were measured using a custom-made TLDA, and the results were normalized to 18S RNA expression. D, T1317 mediates its effects via LXR $\beta$  in dermal fibroblasts. The relative gene expression levels of Mmp3, Mmp13, and Il1 $\beta$  in *ex vivo* cultured LXR $\beta$  WT and KO mice dermal fibroblasts with or without T1317 (1  $\mu$ M) treatment are presented. E, Mmp2 and Mmp9 expression in LXR $\beta$ -null skin. The mRNA expression of Mmp2 and Mmp9 was examined by real-time RT-PCR in LXR $\beta$  WT (white bars) and KO (black bars) skin samples. \*,  $P < 0.01$ ; \*\*,  $P < 0.05$  vs. vehicle or WT control as determined by Student's *t* test.

lipid synthesis (7–9, 11, 28, 29). Here, we demonstrate that T1317 induced the expression of the keratinocyte early differentiation marker involucrin (IVL) as well as late differentiation markers loricrin (LOR), filaggrin (FLG), and transglutaminase 1 (TGM1) in NHEKs (Fig. 3A). The LXR ligand may induce the expression of these genes indirectly by augmenting keratinocyte differentiation via increased AP-1 activity because it increased the expression of IVL via its upstream AP-1 motif (26, 30–33). We next examined the effect of LXR $\beta$  ablation on the expression of these differentiation markers and Tgm family members. As shown in Fig. 3B, the expression of Iv1, Tgm3, and Tgm6 was down-regulated in LXR $\beta$  KO mouse skin, thus indicating that Iv1 and these Tgm family members are indeed LXR-responsive genes. The LXR ligand also induced the expression of Tgm1 (Fig. 3C), Tgm3,

and Tgm6 (Fig. 3D) in LXR $\beta$  WT but not KO cultured keratinocytes, indicating that T1317 mediated its effects on keratinocyte differentiation markers specifically through LXR $\beta$ .

#### LXR-Mediated Regulation of Lipid Synthesis and Transport Genes in Keratinocytes

A comparison of chronologically aged and young skin shows a significant decrease in total lipid content with aging (7, 28, 29). Because lipids mediate epidermal barrier homeostasis, we next examined the effect of T1317 on the expression of genes involved in fatty acid synthesis and lipid transport. The LXR ligand induced the expression of genes involved in fatty acid synthesis, namely SREBF1, SREBF2, FASN, and SCD, and genes involved in cholesterol and phospholipid trans-

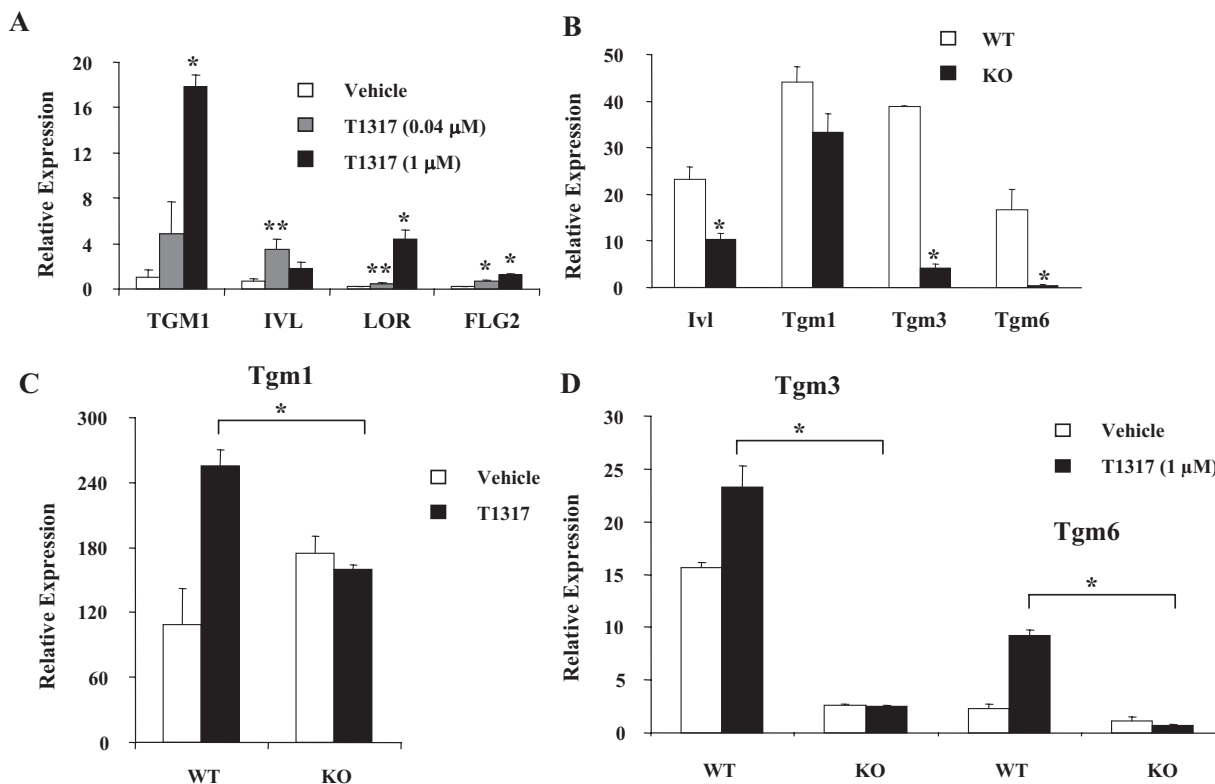


**Fig. 3.** The Effect of T1317 on Markers of Keratinocyte Differentiation

A, The LXR ligand induces keratinocyte differentiation markers in NHEKs. The relative expression level of TGM1, IVL, LOR, and FLG2 was measured by real-time RT-PCR. B, The relative expression of epidermal differentiation markers Ivl, Tgm3, and Tgm6 in LXR $\beta$  WT (white bars) and KO (black bars) mouse skin is presented. C and D, The effect of T1317 (1  $\mu$ M) on Tgm1, Tgm3, and Tgm6 expression in LXR $\beta$  WT and KO keratinocytes was evaluated by quantitative RT-PCR. White bars represent cells with vehicle treatment, and black bars show gene expression in T1317-treated (1  $\mu$ M) mouse keratinocytes. \*,  $P < 0.01$ ; \*\*,  $P < 0.05$  vs. vehicle or WT control as determined by Student's  $t$  test.

port, namely APOE, APOD, ABCG1, ABCA1, ABCA12, ABCA2, and ABCA13 (Fig. 4A). ABCA2, ABCA12, and ABCA13 are newly identified LXR-responsive genes, and the responsiveness of ABCA12 has only recently been described (34). Furthermore, T1317 increased the expression of Abcg1 and Scd1 in LXR $\beta$  WT but not KO keratinocytes (Fig. 4B), indicating that the ligand mediated its effects through LXR $\beta$ .

Ceramides, one of the major lipids in differentiated keratinocytes, play a pivotal role in skin barrier formation (7, 28), and their content declines due to reduced ceramide synthase (LASS) and sphingomyelin phosphodiesterase (SMPD) activities in chronologically aged skin (29). Serine palmitoyltransferase (SPTLC) catalyzes the formation of sphinganine from serine and palmitoyl-CoA (Fig. 4C). Ceramide is produced either from sphinganine or sphingomyelin by LASS or SMPD activities (Fig. 4C). Here, we demonstrate that T1317 induced the expression of LASS4 and SMPD2 in both mock-exposed and UV-exposed NHEKs, whereas its effect on SMPDL3B was observed only in UV-exposed cells (Fig. 4D). Note that UV significantly decreased the expression of LASS4 and SMPD2, and the LXR ligand reversed this effect (Fig. 4D). To confirm the receptor

specificity, the expression of these genes was compared in LXR $\beta$  WT and KO mouse cultured keratinocytes and whole skin. The expression of LASS4, Smpd1, Smpd2, and Smpdl3b was significantly decreased in LXR $\beta$  KO keratinocyte (Fig. 4E) and skin samples (Fig. 4F), demonstrating that LASS and SMPDs are novel LXR-dependent genes.

#### LXR $\beta$ -Null Mouse Is a Model of Human Aged Skin

The effect of LXR ligand on the expression of genes involved in keratinocyte differentiation and barrier formation prompted us to examine the consequences of LXR $\beta$  ablation on mouse skin. LXR $\beta$  KO mice showed reduced epidermal thickness due to decreased keratinocyte proliferation (22). We compared LXR $\beta$  KO and WT skin by transcription profiling using Affymetrix GeneChip arrays. Pathway analysis using a modified version of the sigpath algorithm (35) was used to identify significantly regulated gene sets between LXR $\beta$  KO and WT mouse skin. This analysis revealed a striking resemblance with a previously described gene expression pattern of young vs. aged human skin (36). Genes that were down-regulated in aged

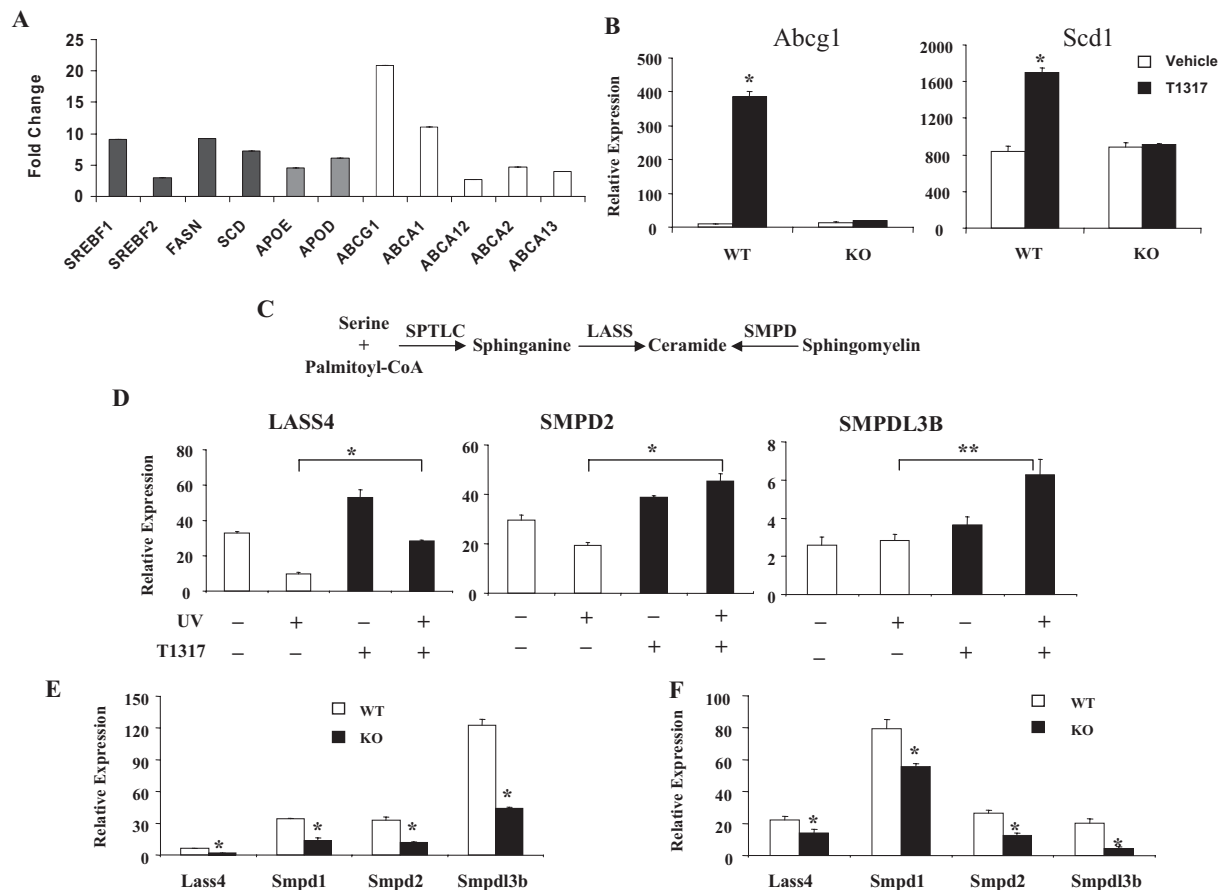


**Fig. 4.** T1317 Induces the Expression of Lipid Synthesis and Transport Genes in Keratinocytes

A, The relative expression of genes involved in fatty acid synthesis (*black bars*), cholesterol binding (*gray bars*), and lipid transport (*white bars*) after treatment of NHEKs with T1317 ( $1 \mu\text{M}$ ) was measured by real-time PCR. B, The effect of T1317 ( $1 \mu\text{M}$ ) on the relative gene expression levels of *Abcg1* and *Scd1* in *ex vivo* cultured LXR $\beta$  WT and KO mice epidermal cells is presented. *White* and *black bars* represent the relative gene expression levels in vehicle and T1317-treated keratinocytes, respectively. C, A schematic representation of ceramide biosynthetic pathway and the enzymes involved is shown. D, The effect of T1317 ( $1 \mu\text{M}$ ) treatment (24 h) on the expression of LASS4, SMPD2, and SMPDL3B in NHEKs with or without UVB exposure ( $8 \text{ mJ/cm}^2$ ) as measured by real-time RT-PCR is shown. Vehicle- and T1317-treated groups are shown as *white* and *black bars*, respectively. E and F, The relative expression of *Lass4*, *Smpd1*, *Smpd2*, and *Smpd3b* in LXR $\beta$  WT (*white bars*) and KO (*black bars*) in mouse keratinocytes (E) and whole skin (F) is shown as measured by real-time RT-PCR, normalized to 18S RNA gene. \*,  $P < 0.01$ ; \*\*,  $P < 0.05$  vs. vehicle or WT control as determined by Student's *t* test.

human skin also showed reduced expression in LXR $\beta$  KO mouse skin (Fig. 5A), thus indicating that LXR $\beta$ -null mouse is a potential model of chronologically aged human skin.

To further characterize the molecular changes in LXR $\beta$  KO, we examined the expression of specific genes associated with skin aging and cell senescence. Because fibroblasts affect keratinocyte proliferation and differentiation, and senescent fibroblasts exhibit reduced cholesterol efflux (37), the expression level of genes involved in lipid efflux/transport was compared in LXR $\beta$  WT and KO fibroblasts. Despite the presence of LXR $\alpha$ , the basal expression of lipid transporters (*Abca1* and *Abcg1*) and cholesterol binding proteins (*ApoD* and *ApoE*) was reduced in LXR $\beta$ -null fibroblasts (Fig. 5B), indicating that KO fibroblasts may exhibit the senescent phenotype because of reduced cho-

lesterol clearance, which is observed in Werner syndrome (human premature aging disorder) fibroblasts (37). Increased COX-2 expression and PGE2 synthesis are reported in photoaged and chronologically aged skin (12), and PGE2 has been linked to replicative senescence in fibroblasts (10). Therefore, we next compared the expression of COX-2 (*Ptgs2*) in LXR $\beta$  WT and KO fibroblasts. As shown in Fig. 5B, *Ptgs2* expression was significantly up-regulated in LXR $\beta$ -null fibroblasts, suggesting that LXR ligands may reverse aging-associated fibroblast senescence. In addition, the expression of MMP2 and MMP9 was also induced in LXR $\beta$  KO skin (Fig. 2E), a feature shared with both photoaged and chronologically aged skin (2, 38). Taken together, these results indicate LXR $\beta$ -null mouse as a model of human aged skin at a genetic level.

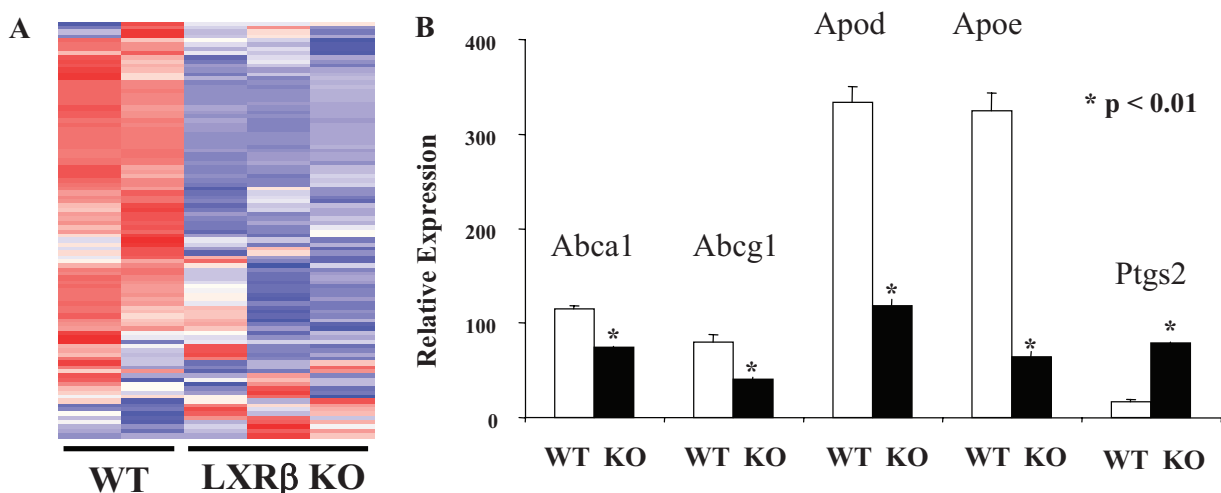


**Fig. 5.** Molecular Defects in LXR $\beta$  KO Skin

A, The relative mRNA expression of a gene set in mouse LXR $\beta$  WT (n = 2) and KO (n = 3) skin identified as regulated in human old age skin compared with human young skin (36). Each lane represents gene set data obtained from one mouse skin sample. The data are visualized in Spotfire 8.0. Each gene is z-scored, normalized, and color-coded (*red*, relatively high expression; *white*, median expression; *blue*, low expression). B, The relative expression of Abca1, Abcg1, Apod, Apoe, and Cox-2 was measured by real-time PCR in LXR $\beta$  WT (*white bars*) and KO (*black bars*) dermal fibroblasts obtained from mice pups. \*,  $P < 0.01$  vs. WT control as determined by Student's *t* test.

### LXR Ligand Inhibits UV-Induced Skin Thickening and Wrinkle Formation *in Vivo*

We next examined whether the molecular changes induced by the LXR ligand can indeed influence the appearance of photoaged skin in an animal model. Therefore, the effect of T1317 was examined on UV-induced skin thickening and wrinkle formation in a hairless albino mouse model (39). UV radiation resulted in a time-dependent increase in skin thickness at wk 2, 4, and 6 in UV-exposed, vehicle-treated mice compared with the mock-exposed groups (Fig. 6A). Topical treatment with T1317 significantly reduced UV-induced abnormal skin thickness in a dose-dependent manner, and T1317 at 10 mM concentration did not show any statistically significant ( $P < 0.05$ ) difference in skin thickness between the UV-exposed (UV+) and mock-exposed (UV-) groups (Fig. 6A). UV exposure of hairless mice for 6 wk also resulted in the appearance of prominent wrinkles in vehicle-treated group in comparison with mock-exposed groups, as shown by silicon rubber replicas of the mouse dorsal skin (Fig. 6B). Quantitation by replica scans showed an increase in wrinkle score in the UV-exposed, vehicle-treated group (Fig. 6C). Remarkably, a significant decrease in wrinkle score was observed at all three doses of the LXR ligand (Fig. 6, B and C). At both 1 and 10 mM concentrations, the wrinkle scores in UV+ groups were not significantly different ( $P < 0.05$ ) from the UV- groups (Fig. 6C). The results from this murine model of photoaging indicate that the LXR ligand indeed inhibits the signs of photo-damage *in vivo*.

### DISCUSSION

This study provides the first evidence demonstrating LXR as a potential therapeutic target for the prevention and treatment of photoaging and chronological skin aging. LXR ligands may show efficacy in these indications because T1317 1) reduced the expression of cytokines and metalloproteinases in UV-activated epidermal keratinocytes and TNF $\alpha$ -activated dermal fibroblasts, 2) increased the expression of keratinocyte differentiation markers, 3) increased the expression of genes required for fatty acid synthesis in keratinocytes, 4) increased the expression of cholesterol binding proteins and lipid transporters in skin cells and 5) increased the expression of enzymes involved in ceramide synthesis in keratinocytes.

Fueled by an increase in the aging population, demand for products and procedures that mitigate the signs of skin aging has increased considerably in recent years. Baby-boomers are demanding products not only to maintain youthful appearance but also to reverse age-related changes. Skin aging is a result of the superposition of two biological processes, chronological aging and photoaging. Currently, there are no prescription treatments for chronologically aged skin, whereas retinoids are the only class of topical prescription agents approved for treating photodamaged skin (40). However, retinoid use is associated with local side effects, such as irritation, erythema, dryness, burning, scaling, and pruritis (40). These properties may further exacerbate the dryness and scaling associated with chronologically aged skin and preclude their use for aged facial skin. Other treatment

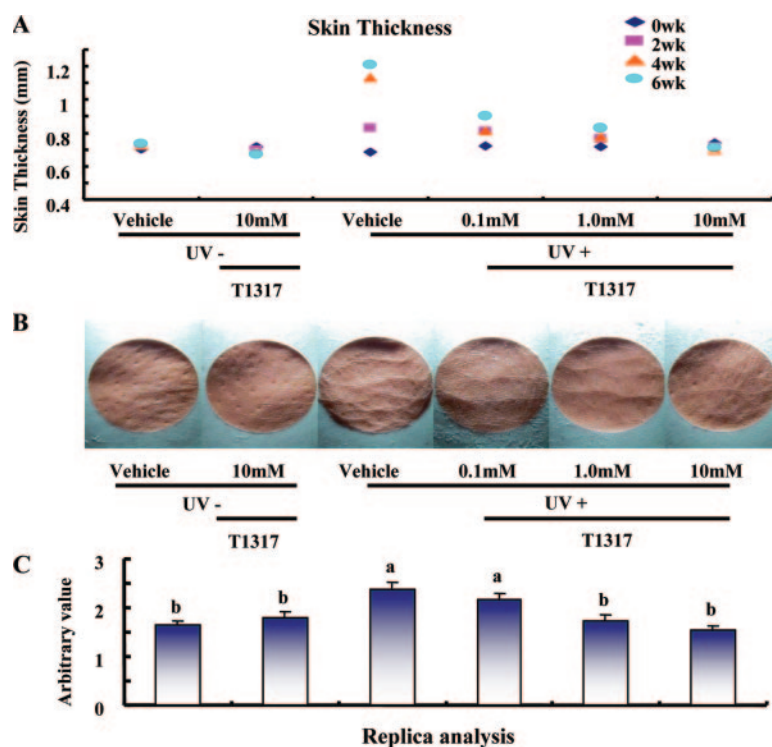


**Fig. 6.** Topical Application of T1317 Shows Efficacy in a Murine Model of Photoaging

A, A time-course of UV radiation effect on hairless mouse skin thickness and the effect of various concentrations (0.1, 1, and 10 mM) of T1317 on skin thickness after 0, 2, 4, and 6 wk of topical treatment is shown. The mice were either mock irradiated or exposed to UV radiation three times a week. The UV dose was increased weekly by 1 MED (1 MED = 100 mJ/cm<sup>2</sup>) to a maximum of 4 MED and subsequently maintained at this level for the remainder of the study period (39). Thickness of the dorsal skin was measured using a caliper at baseline (wk 0) and after 2, 4, and 6 wk of UV exposure. The values are the mean of a total of eight mice per group. B and C, Wrinkle formation was assessed after 6 wk UV exposure by preparing skin replicas (B) and measured quantitatively by computer scanning of the replicas (C). Representative photographs taken at wk 6 are shown. Values represent the mean  $\pm$  SEM ( $n = 5$ ). a, Groups that were statistically significantly different ( $P < 0.05$ ) from those labeled b; b, groups that were not significantly different ( $P < 0.05$ ) from each other.

modalities, such as botulinum toxins and hyaluronic acid fillers, are painful, invasive, and expensive. Thus, there is an unmet need for agents that are safe and efficacious for both photodamaged and chronologically aged skin. Human skin expresses a number of NRs (RARs, VDR, glucocorticoid receptor, PPARs, etc.), and their ligands (retinoids, vitamin D compounds, glucocorticoids, etc.) are important regulators of dermal physiology and pathology. Retinoids function in photoaging, psoriasis, and acne thorough RARs that are expressed in skin (41). Natural and synthetic VDR ligands are used in clinics for the treatment of psoriasis, and glucocorticoids are the treatment of choice for dermal inflammatory indications (41, 42). The emerging biology of PPARs and LXRs in inhibiting cutaneous inflammation and enhancing epidermal barrier function suggests their ligands as potential therapeutics for various dermal indications (21–23, 34, 43, 44).

The etiology of photoaging involves UV insult on keratinocytes, resulting in the expression of NF- $\kappa$ B-responsive cytokines that activate fibroblasts and also mediate the recruitment of neutrophils to the dermis

(3, 4, 45). Cytokine-activated fibroblasts and neutrophils secrete NF- $\kappa$ B and AP-1-dependent MMPs (MMP1, -2, -3, and -9), which degrade the dermal matrix of collagen and elastin. Notably, LXR agonists inhibit NF- $\kappa$ B-mediated gene expression, implicating LXR-NF- $\kappa$ B cross talk as the central basis for their antiinflammatory activity in macrophage systems (46). Therefore, the LXR ligand appears to attenuate cytokine and MMP expression in activated skin cells and may mediate its efficacy in models of photoaging via antagonism of NF- $\kappa$ B-dependent gene expression. In support of this notion, the NF- $\kappa$ B pathway has also been validated as a target for photodamage because a specific pharmacological inhibitor, parthanolide, exhibited efficacy in a murine model of photoaging (45). Interestingly, both UV and cytokine exposures resulted in the attenuation of LXR signaling pathway in skin cells (Fig. 1, D–F), suggesting that the downmodulation of LXR-responsive genes may also contribute to the etiology of photoaging. Accordingly, activation of LXRs by a specific agonist improved photodamage and wrinkle formation in a murine model of photoaging (Fig. 6, A–C). Increased expression of



MMPs is a common mechanism underlying the etiology of both photoaging and chronological skin aging. In both forms of aging, the dermis becomes thin because of increased collagen degradation due to elevated fibroblast MMP production and a concomitant decrease in TIMP-1 and collagen expression as a result of cell senescence (47, 48). Therefore, LXR agonist may also show efficacy in chronologically aged skin by reducing MMPs and increasing TIMP-1 expression in dermal fibroblasts. Cutaneous inflammation is also widely accepted as an etiology of chronological skin aging (49), and a molecular level proof-of-concept was provided by a recent report that identified NF- $\kappa$ B as the major motif associated with aging (50). Adler *et al.* (50) showed that inducible genetic blockade of NF- $\kappa$ B signaling for just 2 wk reversed the gene expression profile of chronologically aged murine epidermis to that of the young mice, suggesting that inhibition of NF- $\kappa$ B-dependent gene expression in the epidermis could not only prevent but also reverse skin aging. Therefore, LXR ligand may show efficacy in chronologically aged skin via its anti-NF- $\kappa$ B activity.

Xerosis or dry skin is the foremost uncomfortable manifestation of the chronologically aged skin, which occurs as a result of reduced lipid synthesis. Interestingly, sphingolipids, fatty acids, and cholesterol content of the aged skin is significantly reduced in comparison with young human and murine skin, leading to defective barrier repair (7, 28, 29). Because skin dehydration is one of the most common causes of fine skin wrinkling (51), the enhancement of epidermal barrier function via increased corneocyte differentiation and keratinocyte lipid generation may contribute to prevention of transepidermal water loss and improvement in skin wrinkling (11). Topical application of LXR ligands inhibited transepidermal water loss and stimulated the synthesis of epidermal cholesterol, fatty acids, and sphingolipids in hairless mouse (23). T1317 also induced the expression of keratinocyte enzymes involved in ceramide biosynthetic pathway (Fig. 4, D and E). The identification of LASS4, SMPD1, SMPD2, and SMPDL3b as newly identified LXR-responsive genes (Fig. 4, D and E) provides a molecular basis for the LXR ligand-mediated increase in sphingolipid synthesis *in vivo* (23). LXR ligands may also increase lipid loading into the lamellar bodies by inducing the expression of lipid binding proteins and ABC transporter family members required for cholesterol and lipid efflux (Fig. 4, A and B). In accordance, LXR ligands are documented to induce the expression of lipid synthesis, binding, and transport genes in liver, macrophage, and microglial systems (16, 19). Furthermore, LXR ligands also induced the expression of ABCA1 in human keratinocytes and murine epidermis (25). Therefore, LXR ligands may exhibit a potent antixerosis therapeutic effect, thus alleviating one of the major symp-

toms of aged skin that leads to the deterioration of epidermal barrier function and initiation of other serious cutaneous conditions, *e.g.* dermatitis/eczema, which is observed at an increasing incidence with advancing age (52). Furthermore, we have identified two new members of the ABC family, namely, ABCA2 and ABCA13, that show LXR-dependent increase in their expression in keratinocytes (Fig. 4A). However, whether these transporters are localized on the lamellar bodies and the identity of lipids that ABCA2, ABCA12, and ABCA13 transport are open questions and need to be answered to fully understand the LXR mechanism of action in lipid transport and lamellar body loading.

There is a defect in keratinocyte terminal differentiation in aged skin. Oxysterols increase cornified envelope formation and the expression of TGM1 and IVL in keratinocytes (31), and the enhanced expression of IVL has been attributed to the induction of Jun/Fos family members (26, 31). Here, we demonstrate that TGM1, IVL, LOR, and FLG are LXR-responsive genes in NHEKs because their expression was induced by T1317 (Fig. 3A). *Tgm1*, *Tgm3*, *Tgm6*, and *Ivl* are plausibly direct LXR-responsive genes because their expression was decreased in LXR $\beta$  KO mouse skin (Fig. 3B). LXR-mediated induction of AP-1-responsive LOR and FLG expression might be secondary to enhanced keratinocyte differentiation and/or increased cholesterol sulfate-protein kinase C  $\alpha$  signaling via induction of cholesterol sulfotransferase expression (43). Therefore, LXR ligands may normalize the keratinocyte terminal differentiation defect that is observed in the aged epidermis (11).

Importantly, LXR $\beta$ -null mice showed epidermal thinning because of decreased keratinocyte proliferation (22), which is a phenotypic hallmark of chronologically aged skin. Dermal fibroblasts also exhibit senescent phenotype in chronological skin aging (10, 48). Enhanced PGE2 production as well as COX activity has been associated with the underlying pathology of various disorders of aging, such as atherosclerosis, arthritis, autoimmunity, and cancer. Increased UV-mediated COX-2 expression is reported in aged human skin, and it has been implicated to play a role in fibroblast senescence (10, 12). Augmentation of COX-2 activity in aged human skin assumes importance because PGE2 has been shown to inhibit collagen and fibronectin synthesis and enhance MMP production in fibroblasts (10). Importantly, a selective COX-2 inhibitor reduced senescence-associated PGE2 production and COX-2, p53, and MMP-1 expression and enhanced the expression of TIMP-1 and procollagen in dermal fibroblasts (10). Interestingly, COX-2 expression was up-regulated in LXR $\beta$  KO fibroblasts (Fig. 5B), indicating a molecular similarity between LXR $\beta$ -null mouse and human aged skin fibroblasts. Therefore, LXR ligands may also impact the process of skin aging by inhibiting the negative consequences of increased PGE2 via down-regulating the expression of

COX-2 in fibroblasts. Dermal fibroblasts from Werner syndrome, a human premature aging disorder, patients show an early onset of senescent phenotype, which has been linked to defective cholesterol efflux and intracellular lipid transport (37). LXR $\beta$ -null fibroblasts demonstrated decreased expression of cholesterol efflux and binding proteins, thus indicating that LXR ligands may reverse aging-associated fibroblast senescence by normalizing lipid homeostasis (Fig. 5B). Decreased expression of lipid transport proteins in LXR $\beta$  KO mice and Werner syndrome fibroblasts may result in not only increased intracellular lipid accumulation but also enhanced UVA-induced lipid peroxidation, which is observed in skin aging (14). Significantly, transcriptional profiling of LXR $\beta$  KO vs. WT skin showed similar regulation of a subset of genes (Fig. 5A) with a previously described transcriptional profiling study comparing human aged vs. young skin (36), further corroborating LXR $\beta$  KO to be a model of human aged skin at both phenotypic and molecular levels.

In the past century, medical advances have gradually augmented the average life expectancy throughout the world, which in turn has increased the human desire to remain youthful. Because the face plays an important role in our daily communications, it is currently the focus of anti-skin aging cosmaceuticals and therapeutics. The clinical development of potent and efficacious products for the face is likely to spur research for the identification of safe compounds for the thickening and restoration of the whole body skin, *i.e.* an efficacious agent for skin fragility, bedsores, and other less understood and intractable ailments of the aged skin. Currently, we are at an early stage of skin anti-aging research, and understanding the mechanism of action of therapeutically effective facial agents will help in our efforts to identify novel molecules to rejuvenate aged senescent keratinocytes and fibroblasts, which may pave the way for the identification of agents that increase the lifespan by reversing the clock for multiple cell types and tissues.

## MATERIALS AND METHODS

### Skin Cells and Cell Culture Conditions

NHEKs and NHDFs (Cambrex/Lanza, Walkersville, MD) and human dermal fibroblasts cell lines HFF and BJ-5ta (American Type Culture Collection, Rockville, MD) were cultured as per vendors' recommendations. In general, cells were trypsinized and seeded on d 0, T1317 treatments (0.4 or 1  $\mu$ M) were done on d 1 with and without UV (8 mJ/cm<sup>2</sup>) or TNF $\alpha$  (1 ng/ml) activations, and cells were harvested on d 2 with lysis buffer (Applied Biosystems/Ambion, Foster City, CA) directly added to the cultured cells after a PBS wash. Cells were either used for RNA purification using QIAGEN RNeasy RNA purification column (QIAGEN, Hilden, Germany) as per vendor's protocol or directly processed to cDNA using Cell-to-cDNA lysis buffer (Ambion, Foster City, CA).

### Expression Profiling

The expression of LXR $\alpha$  and  $\beta$  was interrogated in various tissues by *in silico* mining of Wyeth Research database of Human Genome U133 Plus 2.0 transcriptional profiling data from 33 normal human tissues. The data were acquired from a source generated by Gene Logic (Gaithersburg, MD) and Wyeth Research (Cambridge, MA) using standardized procedures and internal controls to minimize variation. Each tissue consisted of at least six replicates. All transcriptional profiling data were normalized to a mean signal intensity value of 100 in GCOS (Affymetrix, Santa Clara, CA).

### Microarray Processing

Five micrograms of total RNA from whole skin section of LXR $\beta$  KO and WT animals were used to generate biotin-labeled cRNA using an oligo T7 primer in a reverse transcription reaction followed by *in vitro* transcription reaction with biotin-labeled UTP and CTP. Ten micrograms of cRNA were fragmented and hybridized to MOE430 2.0 arrays (Affymetrix). Statistical identification of significantly regulated biological pathways was implemented using a modified approach (35).

### LXR $\beta$ WT and KO Skin Cell Preparations

LXR- $\beta$  KO mice were obtained from Deltagen (San Carlos, CA) in the 129 strain and backcrossed for seven generations into black C57BL/6J mice. LXR- $\beta$  KO was accomplished using LXR- $\beta$  gene sequence deletion from bases 226–395 by using a homologous recombination vector (Deltagen). Skins from newborn mice (2–3 d old) were isolated and floated on 2.5 mg/ml dispase (Invitrogen/GIBCO, Carlsbad, CA) overnight at 4 C and separated into epidermal and dermal layers using small forceps. The epidermal and dermal layers were minced and subjected to several differential centrifugations, fractionations, and filtrations as previously described (53). These cells were then cultured in Eagle's MEM containing fetal bovine serum (8%) in 24-well culture plates (d 0). Cells were treated with vehicle or T1317 on d 2, followed by isolation and purification of RNA on d 3 using RNeasy column (QIAGEN). Gene expression profiles were analyzed using TaqMan low-density array (TLDA) and individual TaqMan gene assays (Applied Biosystems, Foster City, CA).

### Custom-Designed TLDA and Quantitative RT-PCR

The RNA or cDNA obtained from the compound-treated cells were used in custom-designed TLDA or individual TaqMan assays (Applied Biosystems) as per vendor's protocols using ABI 7900HT real-time PCR machine. The level of expression was calculated based on the PCR cycle number (Ct), and the relative gene expression level was determined using the  $\Delta\Delta$ Ct method as described elsewhere (54). One TLDA was designed with oligo probes and primer pairs for TNF $\alpha$  (Applied Biosystems assay ID Hs00174128\_m1), IL-1B (Hs00174097\_m1), IL-6 (Hs00174131\_m1), IL-8 (Hs00174103\_m1), MMP1 (Hs00233958\_m1), MMP3 (Hs00233962\_m1), MMP9 (Hs00234579\_m1), TIMP1 (Hs00171558\_m1), DCN (Hs00754870\_s1), COL1A1 (Hs00164004\_m1), CCL3 (Hs00234142\_m1), CCL4 (Hs99999148\_m1), CCL5 (Hs00174575\_m1), NOS2A (Hs00167257\_m1), PTGS2 (Hs00153133\_m1), and 18S (Hs99999901\_s1) control gene. The second TLDA contained oligo probes and primer pairs for known LXR-responsive genes as well as some other genes of interest. It contained probes and primer pairs for ACACA (Hs00167385\_m1), ACAT2 (Hs00255067\_m1), APOD (Hs00155794\_m1), APOE (Hs00171168\_m1), FASN (Hs00188012\_m1), FDF1 (Hs00189506\_m1), FOXM1 (Hs00153543\_m1), LDLR (Hs00181192\_m1), NPC1L1 (Hs00203602\_m1), NR1H2 (Hs00173195\_m1), NR1H3

(Hs00172885\_m1), PLTP (Hs00272126\_m1), SCD (Hs00748952\_s1), SLC2A4 (Hs00168966\_m1), SREBF1 (Hs00231674\_m1), SREBF2 (Hs00190237\_m1), STAR (Hs00264912\_m1), ABCA1 (Hs00194045\_m1), ABCA2 (Hs00242232\_m1), ABCA13 (Hs00541549\_m1), ABCG1 (Hs00245154\_m1), ABCA12 (Hs00292421\_m1), ADMTS4 (Hs00192708\_m1), CYP11A1 (Hs00167984\_m1), PTGES (Hs00610420\_m1), MMP1 (Hs00233958\_m1), and housekeeping genes GAPDH (Hs00266705\_g1) and 18S (Hs99999901\_s1). Some of these individual gene assays from the list above (identical assay ID) were also purchased from Applied Biosystems and used for confirmation or focused assay purposes. Other gene assays used in this study included human genes LASS2 (Hs00604577\_m1), LASS4 (Hs01001661\_m1), SMPD1 (Hs00609415\_m1), SMPD2 (Hs00162006\_m1), SMPDL3B (Hs00205522\_m1), TGM1 (Hs00165929\_m1), IVL (Hs00846307\_s1), LOR (Hs01894962\_s1), and FLG2 (Hs00418578\_m1) and mouse genes Abcg1 (Mm00437390\_m1), Abca1 (Mm00442646\_m1), Scd1 (Mm00772290\_m1), Mmp2 (Mm00439508\_m1), Mmp3 (Mm00440295\_m1), Mmp9 (Mm00442991\_m1), Mmp13 (Mm00439491\_m1), Il1b (Mm00434228\_m1), Tgm1 (Mm00498375\_m1), Tgm3 (Mm00436999\_m1), Tgm6 (Mm00624922\_m1), Ivl (Mm00515219\_s1), Smpd1 (Mm00488318\_m1), Smpd2 (Mm00486247\_m1), Smpdl3b (Mm00505696\_m1), and Lass4 (Mm00482658\_m1).

### Murine Model of Photoaging

Five-week-old female albino hairless mice (Hos:HR-1) were obtained from the HOSHINO Laboratory Animals (HOS, Kotoh-cho, Japan). Animals had free access to food and water and were acclimated for 1 wk before the study. Eight mice were allocated to each group (total six groups for each test compound). All experimental protocols were approved by Institutional Animal Care and Use Committee of Clinical Research Institute, Seoul National University Hospital (Association for Assessment and Accreditation of Laboratory Animal Care accredited facility). An UV irradiation device that included TL20W/12RS UV lamps (Philips, Eindhoven, The Netherlands) with an emission spectrum between 275 and 380 nm (peak, 310–315 nm), served as the UV source. A Kodacel filter (TA401/407; Kodak, Rochester, NY) was mounted 2 cm in front of the UV lamp to remove wavelengths of less than 290 nm (UVC). Irradiation intensity at the mouse skin surface was measured using an UV meter (model 585100; Waldmann Co., Villigen-Schwenigen, Germany). The irradiation intensity 20 cm from the light source was 0.5 mW/cm<sup>2</sup>.

Initially, we measured the minimal erythema dose (MED) on dorsal skin of mice. MED can be defined as the minimum amount of radiation exposure required to produce an erythema with sharp margins after 48 h. Mice were exposed to UV light three times per week (Monday, Wednesday, and Friday) for 6 wk. The irradiation dose was increased weekly by 1 MED (1 MED = 100 mJ/cm<sup>2</sup>) up to 4 MED and then maintained at 4 MED. UV irradiation was stopped after irradiation for the sixth week. T1317 or its vehicle (70% ethanol, 30% polyethylene glycol) was topically applied to the dorsal area (50  $\mu$ l) after each exposure to UV irradiation (five times per week). Dorsal skin-fold thickness was measured using a caliper (Peacock; Ozaki MFG Co. Ltd., Tokyo, Japan). Skin thickness was measured on wk 0, 2, 4, and 6. Skin wrinkle replicas were obtained with a silicon rubber (Silflo dental impression material; Flexico Developments, Potters Bar, UK) to the backs of unstrained mice. Skin impressions were photographed using a coupling charge system (CCD) video camera and analyzed by Skin-Visiometer SV 600 software (CK Electronic GmbH, Köln, Germany).

### Acknowledgments

M. Patel and J. Gale are kindly acknowledged for the NR cross-reactivity screen of T1317.

Received July 10, 2008. Accepted September 4, 2008.

Address all correspondence and requests for reprints to: Sunil Nagpal, Nuclear Receptors and Dermatology, Women's Health and Musculoskeletal Biology, Wyeth Research, 500 Arcola Road, Collegeville, Pennsylvania 19426. E-mail: nagpals@wyeth.com; or Jin Ho Chung, Laboratory of Cutaneous Aging Research, Department of Dermatology, Seoul National University College of Medicine, Seoul National University, 28 Yongon-dong, Chongno-Gu, Seoul 110-744, Republic of Korea. E-mail: jhchung@snu.ac.kr.

Disclosure Statement: K.C.N.C., Q.S., S.A.J., S.J., W.W., Y.W., M.L., M.R.Y., C.C.T., L.P.F., and S.N. are employed by Wyeth. J.H.C. received grant support (2007–2008) from Wyeth Research. I.G.O. has nothing to declare.

### References

- Makrantonaki E, Zouboulis CC 2007 Molecular mechanisms of skin aging: state of the art. *Ann NY Acad Sci* 1119:40–50
- Fisher GJ, Kang S, Varani J, Bata-Sorgo Z, Wan Y, Datta S, Voorhees JJ 2002 Mechanisms of photoaging and chronological skin aging. *Arch Dermatol* 138: 1462–1470
- Rijken F, Kiekens RC, Bruijnzeel PL 2005 Skin-infiltrating neutrophils following exposure to solar-simulated radiation could play an important role in photoaging of human skin. *Br J Dermatol* 152:321–328
- Fisher GJ, Datta SC, Talwar HS, Wang ZQ, Varani J, Kang S, Voorhees, JJ 1996 Molecular basis of sun-induced premature skin ageing and retinoid antagonism. *Nature* 379:335–339
- Fagot D, Asselineau D, Bernard F 2004 Matrix metalloproteinase-1 production observed after solar-simulated radiation exposure is assumed by dermal fibroblasts but involves a paracrine activation through epidermal keratinocytes. *Photochem Photobiol* 79:499–505
- Makrantonaki E, Zouboulis CC 2007 William J Cunliffe Scientific Awards. Characteristics and pathomechanisms of endogenously aged skin. *Dermatology* 214: 352–360
- Ghadially R, Brown BE, Sequeira-Martin SM, Feingold KR, Elias PM 1995 The aged epidermal permeability barrier. Structural, functional, and lipid biochemical abnormalities in humans and a senescent murine model. *J Clin Invest* 95:2281–2290
- Zettersten EM, Ghadially R, Feingold KR, Crumrine D, Elias PM 1997 Optimal ratios of topical stratum corneum lipids improve barrier recovery in chronologically aged skin. *J Am Acad Dermatol* 37:403–408
- Campisi J 1998 The role of cellular senescence in skin aging. *J Investig Dermatol Symp Proc* 3:1–5
- Han JH, Roh MS, Park CH, Park KC, Cho KH, Kim KH, Eun HC, Chung JH 2004 Selective COX-2 inhibitor, NS-398, inhibits the replicative senescence of cultured dermal fibroblasts. *Mech Ageing Dev* 125:359–366
- Hashizume H 2004 Skin aging and dry skin. *J Dermatol* 31:603–609
- Seo JY, Kim EK, Lee SH, Park KC, Kim KH, Eun HC, Chung JH 2003 Enhanced expression of cyclooxygenase-2 by UV in aged human skin in vivo. *Mech Ageing Dev* 124:903–910
- Kim HH, Cho S, Lee S, Kim KH, Cho KH, Eun HC, Chung JH 2006 Photoprotective and anti-skin-aging effects of eicosapentaenoic acid in human skin in vivo. *J Lipid Res* 47:921–930
- Polte T, Tyrrell RM 2004 Involvement of lipid peroxidation and organic peroxides in UVA-induced matrix metalloproteinase-1 expression. *Free Radic Biol Med* 36: 1566–1574

15. Chawla A, Repa JJ, Evans RM, Mangelsdorf DJ 2001 Nuclear receptors and lipid physiology: opening the X-files. *Science* 294:1866–1870
16. Zelcer N, Tontonoz P 2006 Liver X receptors as integrators of metabolic and inflammatory signaling. *J Clin Invest* 116:607–614
17. Zelcer N, Khanlou N, Clare R, Jiang Q, Reed-Geaghan EG, Landreth GE, Vinters HV, Tontonoz P 2007 Attenuation of neuroinflammation and Alzheimer's disease pathology by liver X receptors. *Proc Natl Acad Sci USA* 104:10601–10606
18. Joseph SB, McKilligan E, Pei L, Watson MA, Collins AR, Laffitte BA, Chen M, Noh G, Goodman J, Hagger GN, Tran J, Tippin TK, Wang X, Lusis AJ, Hseuh WA, Law RE, Collins JL, Willson TM, Tontonoz P 2002 Synthetic LXR ligand inhibits the development of atherosclerosis in mice. *Proc Natl Acad Sci USA* 99:7604–7609
19. Tontonoz P, Mangelsdorf DJ 2003 Liver X receptor signaling pathways in cardiovascular disease. *Mol Endocrinol* 17:985–993
20. Chintalacharuvu SR, Sandusky GE, Burris TP, Burmer GC, Nagpal S 2007 Liver X receptor is a therapeutic target in collagen-induced arthritis. *Arthritis Rheum* 56:1365–1367
21. Fowler AJ, Sheu MY, Schmutz M, Kao J, Fluhr JW, Rhein L, Collins JL, Willson TL, Mangelsdorf DJ, Elias PM, Feingold KR 2003 Liver X receptor activators display anti-inflammatory activity in irritant and allergic contact dermatitis models: liver-X-receptor-specific inhibition of inflammation and primary cytokine production. *J Invest Dermatol* 120:246–255
22. Kömüves LG, Schmutz M, Fowler AJ, Elias PM, Hanley K, Man MQ, Moser AH, Lobaccaro JM, Williams ML, Mangelsdorf DJ, Feingold KR 2002 Oxysterol stimulation of epidermal differentiation is mediated by liver X receptor- $\beta$  in murine epidermis. *J Invest Dermatol* 118:25–34
23. Man MQ, Choi EH, Schmutz M, Crumrine D, Uchida Y, Elias PM, Holleran WM, Feingold KR 2006 Basis for improved permeability barrier homeostasis induced by PPAR and LXR activators: liposensors stimulate lipid synthesis, lamellar body secretion, and post-secretory lipid processing. *J Invest Dermatol* 126:386–392
24. Schultz JR, Tu H, Luk A, Repa JJ, Medina JC, Li L, Schwendner S, Wang S, Thoolen M, Mangelsdorf DJ, Lusting KD, Shan B 2000 Role of LXRs in control of lipogenesis. *Genes Dev* 14:2831–2838
25. Jiang YJ, Lu B, Kim P, Elias PM, Feingold KR 2006 Regulation of ABCA1 expression in human keratinocytes and murine epidermis. *J Lipid Res* 47:2248–2258
26. Schmutz M, Elias PM, Hanley K, Lau P, Moser A, Willson TM, Bikle DD, Feingold KR 2004 The effect of LXR activators on AP-1 proteins in keratinocytes. *J Invest Dermatol* 123:41–48
27. Inomata S, Matsunaga Y, Amano S, Takada K, Kobayashi K, Tsunenaga M, Nishiyama T, Kohno Y, Fukuda M 2003 Possible involvement of gelatinases in basement membrane damage and wrinkle formation in chronically ultraviolet B-exposed hairless mouse. *J Invest Dermatol* 120:128–134
28. Ghadially R, Brown BE, Hanley K, Reed JT, Feingold KR, Elias PM 1996 Decreased epidermal lipid synthesis accounts for altered barrier function in aged mice. *J Invest Dermatol* 106:1064–1069
29. Jensen JM, Förl M, Winoto-Morbach S, Seita S, Schunck M, Proksch E, Schutze H 2005 Acid and neutral sphingomyelinase, ceramide synthase, and acid ceramidase activities in cutaneous aging. *Exp Dermatol* 14:609–618
30. Crish JF, Eckert RL 2008 Synergistic activation of human involucrin gene expression by Fra-1 and p300: evidence for the presence of a multiprotein complex. *J Invest Dermatol* 128:530–541
31. Hanley K, Ng DC, He SS, Lau P, Min K, Elias PM, Bikle DD, Mangelsdorf DJ, Williams ML, Feingold KR 2000 Oxysterols induce differentiation in human keratinocytes and increase AP-1-dependent involucrin transcription. *J Invest Dermatol* 114:545–553
32. Jang SI, Steinert PM 2002 Loricrin expression in cultured human keratinocytes is controlled by a complex interplay between transcription factors of the Sp1, CREB, AP1, and AP2 families. *J Biol Chem* 277:42268–42279
33. Jang SI, Steinert PM, Markova NG 1996 Activator protein 1 activity is involved in the regulation of the cell type-specific expression from the proximal promoter of the human profilaggrin gene. *J Biol Chem* 271:24105–24114
34. Jiang YJ, Lu B, Kim P, Paragh G, Schmitz G, Elias PM, Feingold KR 2007 PPAR and LXR activators regulate ABCA12 expression in human keratinocytes. *J Invest Dermatol* 128:370–377
35. Tian L, Greenberg SA, Kong SW, Altschuler J, Kohane IS, Park PJ 2005 Discovering statistically significant pathways in expression profiling studies. *Proc Natl Acad Sci USA* 102:13544–13549
36. Ly DH, Lockhart DJ, Lerner RA, Schultz PG 2000 Mitotic misregulation and human aging. *Science* 287:2486–2492
37. Zhang Z, Hirano K, Tsukamoto K, Ikegami C, Koseki M, Saijo K, Ohno T, Sakai N, Hiraoka H, Shimomura I, Yamashita H 2005 Defective cholesterol efflux in Werner syndrome fibroblasts and its phenotypic correction by Cdc42, a RhoGTPase. *Exp Gerontol* 40:286–294
38. Chung JH, Seo JY, Choi HR, Lee MK, Youn CS, Rhie G, Cho KH, Kim KH, Park KC, Eun HC 2001 Modulation of skin collagen metabolism in aged and photoaged human skin in vivo. *J Invest Dermatol* 117:1218–1224
39. Park CH, Lee MJ, Kim JP, Yoo ID, Chung JH 2006 Prevention of UV radiation-induced premature skin aging in hairless mice by the novel compound melanocin A. *Photochem Photobiol* 82:574–578
40. Singh M, Griffiths C 2006 The use of retinoids in the treatment of photoaging. *Dermatol Ther* 19:297–305
41. Nagpal S, Chandraratna RA 2000 Recent developments in receptor-selective retinoids. *Curr Pharm Des* 6:919–931
42. Schäcke H, Berger M, Rehwinkel H, Asadullah K 2007 Selective glucocorticoid receptor agonists (SEGRAs): novel ligands with an improved therapeutic index. *Mol Cell Endocrinol* 275:109–117
43. Jiang YJ, Kim P, Elias PM, Feingold KR 2005 LXR and PPAR activators stimulate cholesterol sulfotransferase type 2 isoform 1b in human keratinocytes. *J Lipid Res* 46:2657–2666
44. Nagpal S 2003 An orphan meets family members in skin. *J Invest Dermatol* 120:viii–x
45. Tanaka K, Hasegawa J, Asamitsu K, Okamoto T 2005 Prevention of the ultraviolet B-mediated skin photoaging by a nuclear factor  $\kappa$ B inhibitor, parthenolide. *J Pharmacol Exp Ther* 315:624–630
46. Joseph SB, Castrillo A, Laffitte BA, Mangelsdorf DJ, Tontonoz P 2003 Reciprocal regulation of inflammation and lipid metabolism by liver X receptors. *Nat Med* 9:213–219
47. Zeng G, McCue HM, Mastrangelo L, Millis AJ 1996 Endogenous TGF- $\beta$  activity is modified during cellular aging: effects on metalloproteinase and TIMP-1 expression. *Exp Cell Res* 228:271–276
48. Varani J, Dame MK, Rittie L, Fligel SE, Kang S, Fisher GJ, Voorhees JJ 2006 Decreased collagen production in chronologically aged skin: roles of age-dependent alteration in fibroblast function and defective mechanical stimulation. *Am J Pathol* 168:1861–1868
49. Thornfeldt CR 2008 Chronic inflammation is etiology of extrinsic aging. *J Cosmet Dermatol* 7:78–82

50. Adler AS, Sinha S, Kawahara TL, Zhang JY, Segal E, Chang HY 2007 Motif module map reveals enforcement of aging by continual NF- $\kappa$ B activity. *Genes Dev* 21: 3244–3257
51. Draelos ZD 2007 The latest cosmeceutical approaches for anti-aging. *J Cosmet Dermatol* 6:2–6
52. Choi EH, Man MQ, Xu P, Xin S, Liu Z, Crumrine DA, Jiang YJ, Fluhr JW, Feingold KR, Elias PM, Mauro TM 2007 Stratum corneum acidification is impaired in moderately aged human and murine skin. *J Invest Dermatol* 127: 2847–2856
53. Zheng Y, Du X, Wang W, Boucher M, Parimoo S, Stenn KS 2005 Organogenesis from dissociated cells: generation of mature cycling hair follicles from skin-derived cells. *J Invest Dermatol* 124:867–876
54. Livak KJ, Schmittgen TD 2001 Analysis of relative gene expression data using real-time quantitative PCR and the  $2^{-\Delta\Delta C_T}$  method. *Methods* 25:402–408



*Molecular Endocrinology* is published monthly by The Endocrine Society (<http://www.endo-society.org>), the foremost professional society serving the endocrine community.